ARTICLE OPEN

Check for updates

Magnitude and kinetics of a set of neuroanatomic volume and thickness together with white matter hyperintensity is definitive of cognitive status and brain age

Neha Yadav[1], Niraj Kumar Gupta[1], Darshit Thakar[1] and Vivek Tiwari[1]✉

Even among the subjects classified as cognitively normal, there exists a subset of individuals at a given chronological age (CA) who harbor white matter hyperintensity (WMH) while another subset presents with low or undetectable WMH. Here, we conducted a comprehensive MRI segmentation of neuroanatomic structures along with WMH quantification in groups of cognitively normal (CN), cognitively impaired (CI) individuals, and individuals with an etiological diagnosis of cognitive impairment owing to Alzheimer's Disease (CI-AD) across the early (50–64 years), intermediate (65–79 years), and late (≥80 years) age groups from the NACC cohort. Neuroanatomic volumetry quantification revealed that thinning of the parahippocampal gyrus in the early ($p = 0.016$) and intermediate age groups ($p = 0.0001$) along with an increase in CSF ($p = 0.0009$) delineates between CI and CI-AD subjects. Although, a significant loss of ~5–10% in volume of gray matter ($p_{(CN\ vs\ CI)} < 0.0001$, $p_{(CN\ vs\ CI\text{-}AD)} < 0.0001$), white matter ($p_{(CN\ vs\ CI)} = 0.002$, $p_{(CN\ vs\ CI\text{-}AD)} = 0.0003$) and hippocampus ($p_{(CN\ vs\ CI)} = 0.007$, $p_{(CN\ vs\ CI\text{-}AD)} < 0.0001$) was evident at the early age groups in the CI and CI-AD compared to CN but it was not distinct between CI and CI-AD. Using the neuroanatomic and WMH volume, and the supervised decision tree-based ML modeling, we have established that a minimum set of Three brain quantities; Total brain (GM + WM), CSF, and WMH volume, provide the Optimal quantitative features discriminative of cognitive status as CN, CI, and CI-AD. Furthermore, using the volume/thickness of 178 neuroanatomic structures, periventricular and deep WMH volume quantification for the 819 CN subjects, we have developed a quantitative index as 'Brain Age' (BA) depictive of neuroanatomic health at a given CA. Subjects with elevated WMH load (5–10 ml) had increased BA (+ 0.6 to +4 years) than the CA. Increased BA in the subjects with elevated WMH is suggestive of WMH-induced vascular insult leading to accelerated and early structural loss than expected for a given CA. Henceforth, this study establishes that quantification of WMH together with an optimal number of neuroanatomic features is mandatory to delve into the biological underpinning of aging and aging-associated cognitive disorders.

Translational Psychiatry (2024)14:389 ; https://doi.org/10.1038/s41398-024-03097-2

INTRODUCTION

Chronological aging is one of the major unavoidable risks for brain disorders [1]. While there is overall structural atrophy with chronological aging [2–9], the presence of white matter hyperintensity (WMH) [10] on brain MRI, commonly known as a small vessel disease arising from infarcts in small vessels indicative of fiber loss, is remarkably noticed in a subset of individuals with chronological aging. Given the subtle structural, fiber, and small vessel changes observed with chronological aging, a large fraction of chronological aging-associated structural and vascular changes may overlap with cognitive pathologies, thus complicating the precise clinical delineation of cognitively normal (CN), cognitively impaired (CI) and cognitively impaired subjects with Alzheimer's Disease (CI-AD) at a given chronological age (CA). Aging and aging-associated cognitive disorders are multifactorial events; therefore, till date, there are no definitive in vivo non-invasive quantitative structural and vascular determinants of cognitive status and brain health [11–17]. Brain MRI segmentation provides several neuroanatomic features, but not all the neuroanatomic structural changes are sensitive and suitable for establishing brain health and cognitive status, thus limiting the utility of neuroanatomic volumetry measurements in clinical settings for immediate decision-making. Therefore, identifying a set of minimal but optimal neuroanatomic and cerebrovascular events unique in terms of threshold, sequence of occurrence viz early, intermediate, and late, and its rate of atrophy/hypertrophy/thinning is needed for precise delineation of CN, CI, and CI-AD.

We have observed that even within the subjects classified as CN, a subset of individuals at a given CA presents with high WMH while another subset has low/undetectable WMH [18, 19]. While aging studies in the past have focused on structural alterations, given the distinct WMH load in the aging subjects quantifying the neuroanatomic volumetry together with WMH load will provide a quantitative platform to pinpoint the brain structural health and associated cognitive implications at a given CA. Conventionally, brain health in clinical set up is measured based on cognitive performance. Classification of subjects with WMH as CN indicates a mismatch between cognitive evaluations and the presence of

[1]Indian Institute of Science Education and Research (IISER) Berhampur, Berhampur, India. ✉email: vivekt@iiserbpr.ac.in

Received: 28 July 2023 Revised: 5 September 2024 Accepted: 13 September 2024
Published online: 27 September 2024

structural abnormalities which are detrimental to brain health. WMH load is likely to pose a vascular insult to neuroanatomic structures which beyond a threshold may lead to altered brain health corresponding to subjects without WMH. Therefore, one of the objectives of this study is to quantify WMH load and investigate the threshold and kinetics of WMH with aging together with neuroanatomic volumetry to delve into the plausible impact of WMH on brain structural health and cognition with chronological aging. Therefore, to establish the minimal but optimal number of unique neuroanatomic features and their thresholds unique to cognitive status as CN, CI, and CI-AD, comprehensive quantification of brain structures and WMH, their sequence and temporal order, kinetics and magnitude of alterations with chronological aging have been performed in this study using the cohort from National Alzheimer's Coordinating Center (NACC) (Supplementary Fig. 1).

The comprehensive MRI segmentation of neuroanatomic features together with WMH quantification across the early (50–64 years), intermediate (65–79 years), and late (≥80 years) age groups from the NACC cohort, depicts that a subset of neuroanatomic changes like medial cortical thinning of parahippocampal gyrus together with increase in CSF are discriminative of CI from CI-AD at early age groups. Although a significant loss of gray matter (GM), white matter (WM), and hippocampus was observed at the early age group in CI and CI-AD compared to CN, the loss in GM, WM, and hippocampus lacks sensitivity to discriminate between CI and CI-AD at the early age groups. Using ML modeling for all the neuroanatomic features and WMH load, we have established that a minimum set of Three optimal brain quantities: Total brain (GM + WM), CSF, and WMH volume, are sufficient to provide a significant and optimal discrimination of cognitive status as CN, CI, and CI-AD.

Further, using the neuroanatomic volume/surface area/thickness for 178 MRI-segmented brain structures, periventricular and deep WMH quantification, and CA (50–99 years) in the cohort of CN subjects, we have developed a unique Brain Age (BA) estimation model to determine BA and Brain Age Gap (BAG) relative to the CA as an indicator of neuroanatomic brain health. Indeed, even the subjects classified as CN, when presented with WMH load 5–10 ml, showed increased brain age, suggestive of WMH-induced vascular insult to brain structures.

METHODS

Study population and characteristics

Longitudinal MR Images, clinical investigations, and cognitive status of subjects labeled as CN, CI, and CI-AD were obtained from NACC for the subjects enrolled from 2005 to 2021. NACC is a longitudinal multicenter study established in 1999 by the National Institute of Aging (NIA) which collects and standardizes clinical and neuropathological data from Alzheimer's Disease Research Centers (ADRCs) across the United States [20–22]. The ADRCs obtain the written informed consent from the participants based on the IRB approval of each ADRCs (https://naccdata.org/requesting-data/nacc-data). All NACC data is freely available to researchers. To receive the NACC data a request is submitted by the user (https://naccdata.org/requesting-data/data-request-process). For the present study, we received anonymized Uniform Data Set (UDS) and imaging data (MRI) from the NACC ADRCs (Data Request ID #5530) on 22 October 2021, for our analysis. The cognitive status labeled as CN, CI, and CI-AD is based on the NIAA-NIND criterion employed by NACC as a variable NACCALZD. A total of N = 3058 longitudinal MRI scans were acquired using standard MPRAGE T1-weighted (T1w) and Axial T2-FLAIR methods from the CN, CI, and CI-AD (N = 2114) subjects enrolled in the NACC study till September 2021 from 16 ADRCs (https://www.alz.washington.edu/) were received from NACC.

Only those MRI data obtained within a range of 1-year from the cognitive measurements were included for brain neuroanatomic and white matter hyperintensity (WMH) measurements and further analyses. Hence, the total number of longitudinal MRI scans included in our study from CN, CI, and CI-AD were 2642 (CN = 1616, CI = 252, and CI-AD = 774) arising from subject numbers as $N_{CN} = 1082$, $N_{CI} = 197$, and $N_{CI\text{-}AD} = 588$ (Supplementary Table 1A).

Brain region volumetry thickness quantification and its kinetics with aging across CN, CI, and CI-AD

The MRI-based volumetry and thickness of brain regions were obtained using the Imaging of Dementia & Aging (IDeA) Lab pipeline (Director: Charles DeCarli, MD; University of California, Davis; https://idealab.ucdavis.edu/) for investigating the chronological aging-associated changes in magnitude and kinetics of structural and WMH volume across the CN, CI, and CI-AD subjects. Volume of gray matter (GM), white matter (WM), total brain (BRNV), hippocampus (HP), lateral ventricles (LV), cerebrospinal fluid (CSF), and WMH for the CN, CI, and CI-AD subjects obtained from segmentation using IDeA lab pipeline were normalized with total intracranial volume (ICV) using Eq. (1):

$$V_{norm} = (V_{estimated}/V_{ICV}) \times V_{avg-ICV} \quad (1)$$

V_{norm} denotes normalized volume; $V_{estimated}$ is the volume obtained from segmentation, and $V_{avg\text{-}ICV}$ represents mean ICV was estimated separately for the CN, CI, and CI-AD groups within each age subgroup [23, 24]. Additionally, for medial temporal cortical thickness (parahippocampal gyrus: PHG, entorhinal cortex: EC), the average thickness of the two hemispheres was calculated.

To examine the relationship between the change in brain region volume or thickness with CA in CI and CI-AD relative to the CN group, a Linear Mixed Effect (LME) model [25] (Supplementary Table 4A) was employed on longitudinal MRI measurements using R packages (R 4.1.2, lem4 1.1.35.1, emmeans 1.8.6) [26] and also tested for a linear regression model [27, 28] (Supplementary Table 4B) for the measurements obtained from the first visit of each subject. The models were structured as a function of age, and the intercept was adjusted for 50 years of age (Eq. 2) to account for the various age of entry of the subjects in the study, using the following equation:

$$Age50_{ij} = Age_{ij} - 50 \quad (2)$$

$$\begin{aligned} Y_{ij} = {} & \beta_0 + \beta_1 \times Age50_{ij} + \beta_2 \times (CI \times Age50)_{ij} \\ & + \beta_3 \times CI_{ij} + \beta_4 \times (AD \times Age50)_{ij} \\ & + \beta_5 \times AD_{ij} + Si + \varepsilon_{ij} \end{aligned} \quad (3)$$

In Eq. 3, Y_{ij} represents dependent variables viz the brain region volume or thickness for the ith subject at jth time point modeled as a function of several independent variables such as Age 50, and cognitive status (CI and CI-AD) for the ith subject at jth time point. CI_{ij} and AD_{ij} are binary indicator variables for the CI and CI-AD status of ith subject at jth time point, respectively. The coefficients β_0, β_1, β_2, β_3, β_4, and β_5 are the parameters of the model that represent the fixed effect of each independent variable on the dependent variable (Supplementary Table 4). The intercept β_0 represents the value of the dependent variable at age 50 when all independent variables are equal to zero. The slope β_1 represents the change in the dependent variable per unit change in Age for the control group (CN). The interaction coefficients β_2 and β_4 represent the effects of CI (when CI = 1) and CI-AD (when AD = 1) in addition to the effects of chronological aging, respectively. The β_3 and β_5 coefficients represent the effect of CI (when CI = 1) and CI-AD (when AD = 1), respectively on the brain regions when the age is held constant. S_i represents the random effect for the ith subject. The error term $\varepsilon_{ij} \sim N(0, \sigma^2)$, represents additional variabilities in the dependent variable which may not be explained by the effect of the independent variables.

To quantify the differences in magnitude, MRI-determined volume and thickness for the three cognitive groups from the first of the total visits, were stratified across three age ranges i.e., 50–64 (early), 65–79 (intermediate), and ≥80 (late) as described in prior investigations [29, 30]. A nonparametric multivariate model from the npmv R package [31] was used to test the global differences for the MRI-determined volume and thickness across the CN, CI, and CI-AD across the three age groups.

Kinetics of white matter hyperintensity with age

Segmentation of T2w-FLAIR and T1w images using the IDeA lab pipeline [32] (Director: Charles DeCarli, MD; University of California, Davis; https://idealab.ucdavis.edu/) provided the total WMH volume. The total WMH

volume estimated from the segmentation was normalized by the ICV. An exponential growth curve model using an in-house function (in Python) was fitted and optimized for investigating the kinetics of WMH progression [28] with chronological aging across the three cognitive groups, CN, CI, and CI-AD as follows:

$$WMH = V_0\, e^{r \times Age} \quad (4)$$

Where V_0 is the initial total WMH volume at 50 years of age and r is the rate constant.

Furthermore, the periventricular WMH (PVWMH) and Deep WMH (DWMH) volumes were extracted and estimated from T1-weighted and T2-FLAIR images using a cluster-based fully automated pipeline called "UBO Detector" [33] where UBO stands for Unidentified Bright Object.

Determining optimal number of MRI-obtained brain features for cognitive discrimination

A combination of neuroanatomic volume and thickness of the features that showed significant early/intermediate/late age differences between the cognitive groups together with total WMH volume, age, and gender were used as inputs for machine learning (ML) based supervised analysis (The scikit-learn library [34, 35] in Python) to discern a minimum number of 'Optimal Brain Features' which are discriminative of cognitive status as CN, CI, and CI-AD with higher accuracy and precision. Various decision tree-based supervised ML models: Simple Classification tree [36], Random Forest method [37], Bagging Classification [38, 39], and Extreme Gradient Boosting (XGBoost or XGB) classifier [39, 40] were tested to optimize the number of MRI features discriminative of CN, CI, and CI-AD subjects. The regional brain anatomical volume, cortical thickness, and total WMH volume obtained from the longitudinal measurements from CN, CI, and CI-AD were randomly distributed into training and test sets (80:20). The accuracy and performance of the four-decision tree-based ML models for all the plausible combinations of MRI features were analyzed using a stratified k-fold ($k = 5$) cross-validation technique [41], and was iterated 6 times. Each iteration included a unique subset of the training subjects such that none of the subjects gets repeated in either of the iterations. Furthermore, precision (P), recall score (R), accuracy (A), and confusion matrix were determined to establish the best-suited ML model. The true positive (TP), false positive (FP), and false negative (FN) values obtained from the confusion matrix were used to estimate the P, R, and A using scikit-learn [34].

Estimating the brain age from neuroanatomical structures and WMH

To estimate brain age (BA) as a function of neuroanatomic volumetry and WMH load for a given CA from the cohort of cognitively normal subjects (727 longitudinal MRI scans from 528 subjects). The BA determination ML model was developed using 178 neuroanatomic volumetry, two WMH quantities (PVWMH and DWMH), and CA. Neuroanatomic volumetry segmentation was performed using the automated cortical reconstruction segmentation method (FreeSurfer Version 7.2.0) [42], and WMH load was quantified using the UBO Detector pipeline [33].

The training set involved MRI data from only the CN subjects (221 scans out of 727), who had undetectable or low WMH (PVWMH < 1.5 ml and DWMH < 1.5 ml) load. To rule out the effect of WMH-induced abnormality on brain structures, only the subjects who had undetectable or low WMH were included in the training set for brain age estimation. Bagging and error correction techniques were performed by dividing the training data into numerous train and validation sets, such that each sample serves as a training set at least in one of the trials and validation set in another trial. The training and validation processes were iterated for 50 times. The BA estimation model was developed in Python using the Scikit-learn [34] library.

Subsequently, the trained Brain Age model was used to predict BA and BAG [43] using the following equation.

$$BAG = \text{Chronological Age} - \text{Estimated Brain Age} \quad (5)$$

Furthermore, using the Scikit-learn [34] python library approach, a set of top ten important features decisive of the brain age derived using permutation importance strategy was obtained. The BA estimation model trained using the NACC data was further cross-validated for CN subjects harboring low WMH (0–1.5 ml) and high WMH (5–10 ml) from the ADNI-3 cohort (N = 92).

Statistical analysis

The global differences in neuroanatomic volume (6 neuroanatomic structures: GM, WM, BNRV, HP, LV, CSF), thickness (2 structures: ENT, PHG), and WMH load (1:Total WMH) between CN, CI, and CI-AD at a given age group (50–64, 65–79, and ≥80) was tested using the nonparametric multivariate model using npmv R package [31], a statistical algorithm that provides the F-approximation and permutation p values for four types rank-based tests: ANOVA type, Wilks' Lambda type, Lawley Hotelling type, and Bartlett Nanda Pillai type Henceforth, for multiple comparison using three cognitive status as factor levels and nine structures as response variables, familywise error rate was controlled at $\boldsymbol{\alpha} = 0.05$. Furthermore, a nonparametric relative effect test was performed to evaluate the extent of impact of all the aforementioned 9 MRI quantified features, their probability, and tendency to serve as a determinant of the cognitive status.

In addition, to evaluate differences for each neuroanatomic feature between cognitive groups (CN vs CI, CN vs CI-AD, and CI vs CI-AD) at a given age range, unpaired two-tailed Welch's t test was conducted, and t values were obtained. Bonferroni correction was applied to account for multiple comparisons, thereby the significance threshold for t values was set at $p < 0.017$.

The multivariate LME regression (Eq. 3) for brain region volume or thickness was performed using the lme4 library in R (R 4.1.2, lme4 1.8.3) [26], and the significance of the full model was tested using the f test. The 'p' values < 0.05 were considered significant for the coefficients β_0, β_1, β_2, β_3, β_4, and β_5 obtained from Eq. 3.

The Supervised ML models were trained using various combinations of MRI-derived neuroanatomic structures to discriminate the cognitive status. The trained ML models were evaluated for each combination of brain features using accuracy, precision, and recall analysis to assess the performance of the model in correctly classifying subjects as CN, CI, and CI-AD.

RESULTS

Global neuroanatomic differences and gray matter, white matter, and total brain volume with aging in CN, CI, and CI-AD

The nonparametric global multivariate analysis (ANOVA type) examining the neuroanatomic differences between CN, CI and CI-AD revealed significant differences for volume of GM, WM, BRNV, HP, LV, CSF, thickness of medial temporal lobe cortices (EC and PHG), and WMH volume at the early age ($F = 15.54$, $p = 0$), intermediate age ($F = 29.35$, $p = 0$) and late age groups ($F = 11.17$, $p = 0$) (Supplementary Table 2A, B). All nine neuroanatomic quantities showed a significant global difference between the cognitive groups at an early age.

Segmentation of T1-weighted images from the first MRI visit revealed a progressive loss in gray matter (GM), white matter (WM), and total brain volume with age in all the three cognitive groups; CN, CI, and CI-AD. At the early age group, the GM, WM, and total brain volume were significantly lower in CI and CI-AD subjects compared to the CN (Fig. 1A, C, Supplementary Fig. 2A, B, Supplementary Fig. 3A). The t-map depicts progressive loss in GM and WM with a significant volume reduction in CI and CI-AD subjects at early age groups, marked with the progressive loss with aging (Fig. 1A, Supplementary Fig. 2A). Unpaired two-tailed Welch's t-test showed significant loss in the GM volume in the CI (593.6 ± 25.1 ml, $p_{(CN\ vs\ CI)} < 0.0001$) and CI-AD subjects ($595.6 \pm 31.4$ ml, $p_{(CN\ vs\ CI\text{-}AD)} < 0.0001$) compared to the CN ($622.4 \pm 20.2$ ml) (Fig. 1C, Supplementary Table 3) at early age groups but not at intermediate and late age groups. However, there was no significant difference in the GM volume between CI and CI-AD at any of the three age groups (Fig. 1C, Supplementary Table 3, 5).

The LME model as described in Eq. 3 (Supplementary Table 4A) revealed a loss of 2.1 ml/year of GM volume for CN subjects while a 1.4 ml/year reduction in CI and 1.7 ml/year decline in CI-AD subjects corresponding to a significantly lower slope in CI and CI-AD subjects compared to the CN (Fig. 1E). However, the baseline volume of GM in CI and CI-AD subjects was remarkably lower compared to the CN group as revealed from the intercepts (obtained upon restricting the initial age to 50 years) (GM-

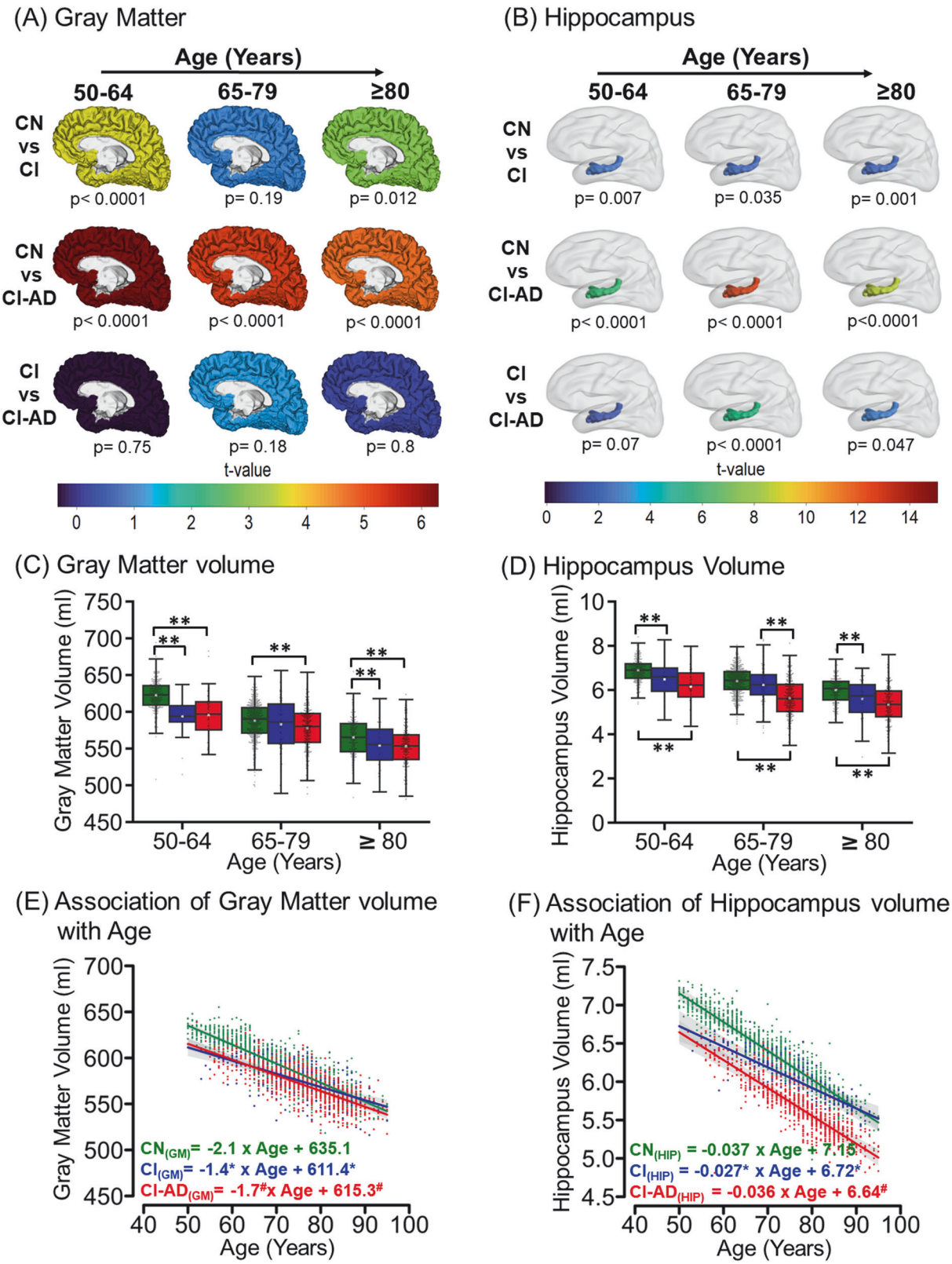

$I_{(CN)} = 635.1$ ml, $I_{(CI)} = 611.4$ ml, $I_{(CI\text{-}AD)} = 615.3$ ml, Intercept-GM: $p_{(CN\ vs\ CI)} < 0.0001$, $p_{(CN\ vs\ CI\text{-}AD)} < 0.0001$, $p_{(CI\ vs\ CI\text{-}AD)} = 0.49$).

Similarly, a significant reduction in WM volume was observed at the early age group for both CI and CI-AD compared to the CN subjects (CN: 495.5 ± 25.1 ml, CI: 473.9 ± 35.1 ml, CI-AD: 476.1 ± 37.6 ml; $p_{(CN\ vs\ CI)} = 0.013$; $p_{(CN\ vs\ CI\text{-}AD} < 0.0001$). The differences between the cognitive groups get masked at intermediate and late age groups (Supplementary Fig. 2B). Moreover, there was no significant difference in WM volume between CI and CI-AD subjects at the early age group

Fig. 1 Magnitude and kinetics of Gray matter and Hippocampus volume with age across CN, CI, and CI-AD subjects. A Gray matter and **B** hippocampus volume of the CN, CI, and CI-AD quantified from the first MRI visit showing the differences between CN vs CI, CN vs CI-AD, and CI vs CI-AD subjects is depicted by the t-map across the three age groups: 50–64 (early) (CN = 300, CI = 29, and CI-AD = 58), 65–70 (intermediate) (CN = 560, CI = 107, and CI-AD = 314), and ≥80 (late) (CN = 222, CI = 61, and CI-AD = 216), wherein warmer color depicts the remarkable difference between the two cognitive groups at the given age range. The significance was set to $p < 0.017$ upon Bonferroni correction. The color bar depicts the *t* value. Boxplot presents the median and mean volume of **C** gray matter and **D** hippocampus quantified from the first visit of the CN, CI, and CI-AD subjects. The volume between the cognitive groups were compared using unpaired, two-tailed Welch's *t* test followed by Bonferroni correction. The upper margin of the boxplot represents the Q3 (third quartile), and the lower margin of the box represents the Q1(first quartile). The height of the box represents the interquartile range (IQR); the median is represented by the black line inside the box and the white square in the middle represents the mean of the sample. Statistical significance for comparing the mean gray matter volume between the cognitive groups (CN, CI, and CI-AD) across the stratified age groups is depicted as $*p < 0.017$, $**p < 0.001$. Linear Mixed Effect (LME) regression model analysis of change in **E** gray matter and **F** hippocampus volume with age. The LME analysis was performed upon setting up the age intercept at 50 years of age for all three cognitive groups. Green, Blue, and Red represent CN, CI, and CI-AD, respectively. Statistical significance for the slope and intercept comparison between CN vs CI (*), CN vs CI-AD ($^{\#}$), and CI vs CI-AD (§) was set at $p < 0.05$.

($p_{(CI\ vs\ CI\text{-}AD)} = 0.8$). The LME model revealed the WM loss with age for the CN group was −3.5 ml/year, while a significantly slower rate of WM loss was observed in the CI (−2.5 ml/year, $p_{(CN\ vs\ CI)} < 0.0001$) and CI-AD (−2.8 ml/year, $p_{(CN\ vs\ CI\text{-}AD)} < 0.0001$) groups compared to CN (Supplementary Table 4A). Moreover, the slope of WM loss was not different between CI and CI-AD groups ($p_{(CI\ vs\ CI\text{-}AD)} = 0.34$) (Supplementary Fig. 2C). Similar to that observed for GM, the baseline volume of WM for CI and CI-AD group was remarkably lower compared to the CN group (WM-$I_{(CN)} = 520$ ml, $I_{(CI)} = 501.1$ ml, $I_{(CI\text{-}AD)} = 504$ ml, Intercept-WM: $p_{(CN\ vs\ CI)} = 0.003$, $p_{(CN\ vs\ CI\text{-}AD)} = 0.0007$, $p_{(CI\ vs\ CI\text{-}AD)} = 0.67$) suggestive of reduced WM in CI and CI-AD subjects.

The Welch's *t*-test showed a significant loss in the total brain volume (BRNV = GM + WM volume) in the CI (1064.9 ± 31.8 ml, $p < 0.0001$) and CI-AD subjects (1071.7 ± 48.6 ml, $p < 0.0001$) compared to the CN (1118.0 ± 27.3 ml). BRNV in the CN group showed a progressive decline with a rate of −5.6 ml/year, while a relatively lower kinetics was observed for the CI (−4.1 ml/year; −27%, $p_{(CN\ vs\ CI)} < 0.0001$) and CI-AD (−4.5 ml/year; −20%, $p_{(CN\ vs\ CI\text{-}AD)} < 0.0001$) groups compared to the CN group (Supplementary Fig. 3B). However, the rates of decline of BRNV were not distinct between CI and CI-AD groups $p_{(CI\ vs\ CI\text{-}AD)} = 0.05$). The intercept analysis clearly depicts BRNV is significantly lower for the CI and CI-AD subjects compared to the CN ($I_{(CN)} = 1155.1$ ml, $I_{(CI)} = 1113.6$ ml, $I_{(CI\text{-}AD)} = 1121.2$ ml, Intercept: $p_{(CN\ vs\ CI)} < 0.0001$, $p_{(CN\ vs\ CI\text{-}AD)} < 0.0001$, $p_{(CI\ vs\ CI\text{-}AD)} = 0.31$) at the baseline (Supplementary Fig. 3B).

Hippocampus volume kinetics with aging in CN, CI, and CI- AD

Indeed, the volume quantification suggests significant hippocampal volume reduction at the early age groups in the CI (CN: 6.9 ± 0.5; CI: 6.4 ± 0.8; $p_{(CN\ vs\ CI)} = 0.007$) and CI-AD (CN: 6.9 ± 0.8; CI-AD: 6.2 ± 0.9; $p_{(CN\ vs\ CI\text{-}AD)} < 0.0001$) compared to the CN subjects. (Fig. 1B, D, Supplementary Table 3, 5). The hippocampus volume was not discriminative of CI and CI-AD subjects at the early age (CI: 6.4 ± 0.8; CI-AD: 6.2 ± 0.9; $p_{(CI\ vs\ CI\text{-}AD)} = 0.07$) while significantly distinct hippocampal volume was observed between CI and CI-AD at intermediate (CI: 6.2 ± 0.8 ml; CI-AD: 5.6 ± 0.9 ml, $p < 0.0001$), age group (Fig. 1B, D). Although the baseline hippocampus volume as depicted by the intercept ($I_{(CN)} = 7.1$ ml, $I_{(CI)} = 6.7$ ml, $I_{(CI\text{-}AD)} = 6.6$ ml) obtained from LME regression was lower for the CI and CI-AD subjects compared to the CN subjects ($p_{(CN\ vs\ CI)} < 0.0001$, $p_{(CN\ vs\ CI\text{-}AD)} < 0.0001$) but the rate of hippocampal loss (CN: −0.037 ml/year; CI: −0.027 ml/year; CI-AD: −0.036 ml/year) with age was similar across the cognitive groups (Fig. 1F).

Medial temporal lobe cortical thinning with aging in CN, CI, and CI-AD

The medial temporal lobe cortices, entorhinal cortex (EC) and parahippocampal gyrus (PHG) exhibited progressive thinning with age for all the cognitive groups as observed on the t-map (Fig. 2A). While the thickness of EC was not distinct between CI and CN at early (CN: 3.60 ± 0.5, CI: 3.48 ± 0.5, $p = 0.2$) and intermediate age groups (CN: 3.65 ± 0.5, CI: 3.49 ± 0.66, $p = 0.019$), the thickness of EC was significantly reduced in the CI-AD subjects at all the age groups compared to CN subjects (Fig. 2A, B; Supplementary Table 3). Noticeably, CI-AD subjects also had reduced EC thickness compared to CI subjects (Fig. 2A, B; Supplementary Table 3) at intermediate and late age groups. Further, the multivariate LME regression (Supplementary Table 4A) of the EC thickness with age for the CN group showed a thinning rate of −0.004 mm/year ($p = 0.02$). The annual reduction of EC thickness with age was ~3 to 4 times faster in CI (−0.012 mm/year) and CI-AD (−0.016 mm/year) subjects compared to the CN subjects ($p_{(CN\ vs\ CI)} = 0.07$, $p_{(CN\ vs\ CI\text{-}AD)} = 0.0001$) despite the baseline thickness of EC was significantly lower for CI-AD subjects compared to CN ($I_{(CN)} = 3.69$ mm vs $I_{(CI\text{-}AD)} = 3.37$ mm, −8.7%, $p_{(CN\ vs\ CI\text{-}AD)} = 0.0002$) and CI subjects ($I_{(CI)} = 3.70$ mm, −8.9%,$p_{(CI\ vs\ CI\text{-}AD)} = 0.01$) (Fig. 2D). However, the per year decrease in the EC thickness was not distinct between CI and CI-AD subjects ($p_{(CI\ vs\ CI\text{-}AD)} = 0.4$) (Fig. 2D).

PHG thinning with age revealed a significantly unique aging pattern, wherein CI-AD subjects exhibit reduced thickness compared to CI at early (CI: 1.91 ± 0.24, CI-AD: 1.78 ± 0.28, $p = 0.016$) as well as intermediate (CI: 1.82 ± 0.32, CI-AD: 1.71 ± 0.29, $p = 0.0001$) age groups (Fig. 2A, C; Supplementary Table 3). Also, the thinning of PHG was discriminative of CI-AD from CN subjects at all the age groups (Fig. 2C). Although the baseline thickness of parahippocampal gyrus for CI-AD subjects was significantly lower by −7.2% compared to CN ($p_{(CN\ vs\ CI\text{-}AD)} = 0.0002$) (Fig. 2E), the yearly rate of PHG thinning was similar across all three cognitive groups (CN: 0.007 mm/year; CI:0.006 mm/year; CI-AD: 0.008 mm/year) (Fig. 2E, Supplementary Table 4A).

Lateral ventricle and CSF volume with aging in CN, CI, and CI-AD

The lateral ventricle and the CSF volume increased significantly with age for all the three cognitive groups (CN, CI, and CI-AD). Interestingly, the mean lateral ventricle volume of CI-AD and CI group was significantly higher compared to CN at the early (CN: 19.2 ± 10.4 ml, CI: 28.1 ± 17.8 ml, CI-AD: 38.0 ± 28.4 ml) and intermediate (CN: 29.2 ± 14.6 ml, CI: 37.3 ± 17.5 ml, CI-AD: 44.3 ± 21.1 ml) age groups. CI and CI-AD did not have significantly different volumes at the early age group, but CI-AD presented with significantly increased ventricular volume compared to CI at the intermediate age group (Fig. 3A, B, Supplementary Table 3). The LME regression analysis for lateral ventricle revealed the annual rate of ventricular increase was similar for all the three cognitive groups, although the intercept for the ventricular volume for CI and CI-AD subjects, was significantly higher compared to the CN ($I_{(CN)} = 12.4$ ml; $I_{(CI)} = 20.1$ ml**;** $I_{(CI\text{-}AD)} = 23$ ml, Intercept: $p_{(CN\ vs\ CI)} = 0.004$, $p_{(CN\ vs\ CI\text{-}AD)} < 0.0001$, $p_{(CI\ vs\ CI\text{-}AD)} = 0.3$) at the baseline age (Fig. 3D, Supplementary Table 4A).

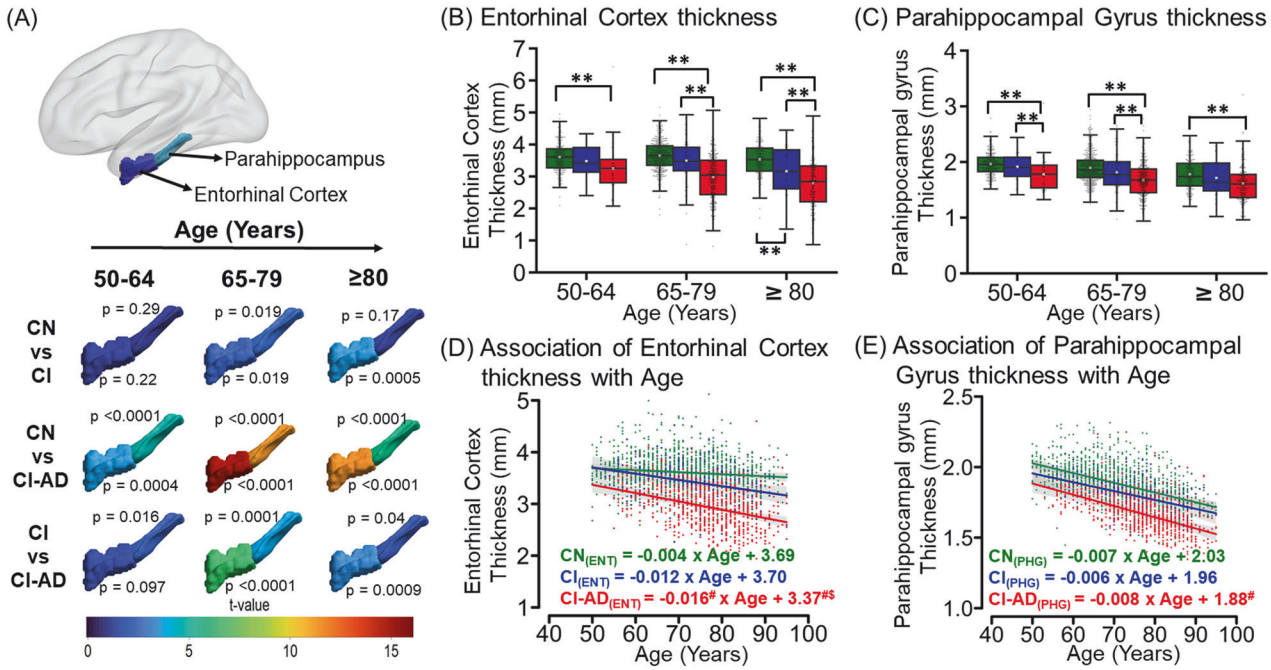

Fig. 2 Cortical thinning with age across CN, CI, and CI-AD subjects. A The t-map depicting the difference of entorhinal cortex thickness and parahippocampal gyrus thickness between CN vs CI, CN vs CI-AD, and CI vs CI-AD across early (CN = 300, CI = 29, and CI-AD = 58), intermediate (CN = 560, CI = 107, and CI-AD = 314), and late (CN = 222, CI = 61, and CI-AD = 216) (CN = 222, CI = 61, and CI-AD = 216) age groups. The significance was set to $p < 0.017$ (Bonferroni corrected) and the color bar depicts the t value. Higher the t value greater the difference between the thickness of cognitive groups. **B**, **C** The Boxplot with median (solid line) and mean (white square) thickness of the entorhinal cortex and parahippocampal gyrus stratified across the early, intermediate, and late age groups for CN (green), CI (blue), and CI-AD (red) subjects. P values were calculated using the unpaired, two-tailed Welch's t test followed by Bonferroni correction. Statistical significance for the mean entorhinal cortex and parahippocampal gyrus thickness comparison among cognitive groups (CN, CI, and CI-AD) across the age groups is depicted as $*p < 0.017$, $**p < 0.001$. **D**, **E** LME regression model analysis of entorhinal cortex and parahippocampal gyrus thickness with age upon setting up the intercept at 50 years. Statistical significance for the slope and intercept comparison between CN vs CI (*), CN vs CI-AD ($^{\#}$), and CI vs CI-AD ($^{\$}$) was set at $p < 0.05$.

The mean CSF volume shows remarkable features, wherein the mean CSF volume was significantly distinct between CI and CI-AD at early age group (CI: 308.6 ± 29.1 ml, CI-AD: 353.9 ± 48.2 ml; $p < 0.0001$) and intermediate age group (CI: 343.4 ± 41.4 ml, CI-AD: 372 ± 37.9 ml; $p < 0.0001$) in addition to significantly higher CSF volume in CI-AD subjects compared to CN subjects across all the three age groups (Fig. 3C, Supplementary Table 3). The multivariate LME regression revealed a significantly slower rate of CSF increase for the CI-AD group (1.5 ml/year) compared to CN (2.4 ml/year, $p_{(CN\ vs\ CI\text{-}AD)} < 0.0001$) and CI (2.4 ml/year, $p_{(CI\ vs\ CI\text{-}AD)} = 0.001$) groups. Furthermore, CI-AD subjects exhibited a significantly higher CSF volume in the CI-AD compared to CN and CI subjects as determined from the intercept ($I_{(CN)} = 280.7$ ml; $I_{(CI)} = 292.2$ ml; $I_{(CI\text{-}AD)} = 333.9$ ml) (Intercept: $p_{(CN\ vs\ CI)} = 0.06$, $p_{(CN\ vs\ CI\text{-}AD)} < 0.0001$, $p_{(CI\ vs\ CI\text{-}AD)} < 0.0001$) at the baseline age (Fig. 3E, Supplementary Table 4A).

White matter hyperintensity with aging in CN, CI, and CI-AD groups

T2-FLAIR segmentation showed that the total WMH load (deep + periventricular WMH) increases with aging across all three cognitive groups (Fig. 4A). With progression in age, a higher WMH load (~2X) was quantified in CI and CI-AD subjects compared to the CN subjects at the early, intermediate, and late age groups (Fig. 4B).

The increase in total WMH with age followed the exponential growth pattern wherein the exponential fitting (Fig. 4C) depicted WMH load increase with age for all the three cognitive groups. The WMH initial load observed at 50 years of age for CN, CI, and CI-AD was $V_{0(CN)} = 1.35$ ml, $V_{0(CI)} = 2.76$ ml, and $V_{0(CI\text{-}AD)} = 2.85$ ml and the rate constant was $r_{(CN)} = 0.063$, $r_{(CI)} = 0.054$, $r_{(CI\text{-}AD)} = 0.049$ respectively suggestive of increased rate of WMH in CI and CI-AD subjects compared to the CN with aging. Indeed, at any given CA the rate of increase of WMH load for CI and CI-AD subjects was ~1.4 times faster (CI/CN: 1.4 ± 0.2; CI-AD/CN: 1.2 ± 0.2) compared to the CN (Fig. 4D). Similarly, WMH quantification from the ADNI cohort, showed a similar rate of increase; ~1.2 times faster (CI/CN: 1.2 ± 0.1; DM/CN: 1.1 ± 0.3) of WMH load for CI and dementia (DM) subjects compared to the CN (Fig. 4E) similar to that observed in the NACC cohort.

ML method for optimizing brain MRI events distinctive of CN, CI, and CI-AD subjects

Using the neuroanatomic volumetry and thickness quantifications, WMH volume estimates together with age, various supervised ML algorithms: simple classification tree, random forest, bagging classification, and XGB classifier (Fig. 5A) were trained to determine the optimal number of brain MRI-segmented features discriminative of cognitive status.

Unique predictive accuracy for the Cognitive status as CN, CI, and CI-AD was observed upon various combinations of neuroanatomic structures and WMH load. Inclusion of only a single neuroanatomic feature provided accuracies ranging between ~50–60%, whereas random addition of various combinations of the volume of neuroanatomic structures with WMH load provided varied accuracies (50–88%) for discrimination of cognitive status (Fig. 5B). A unique combination of two neuroanatomical features *viz* Total Brain Volume and CSF together with WMH volume provided the highest average accuracy (~87 ± 1.3%) discriminative of cognitive status using the XGB Classifier (Fig. 5B, C) and Bagging Classification methods (Fig. 5B). The combination of these three unique MRI-segmented quantities also yielded the highest

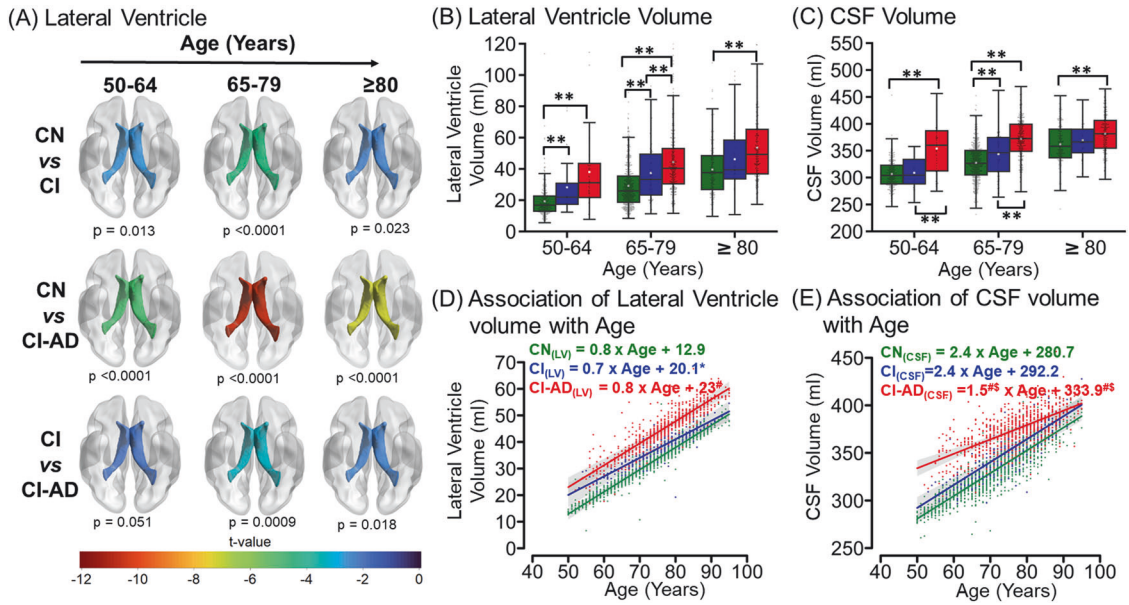

Fig. 3 Lateral Ventricular hypertrophy and CSF increase with age across CN, CI, and CI-AD subjects. A The t-map illustrating the difference of Lateral ventricle volume between CN vs CI, CN vs CI-AD, and CI vs CI-AD across three age groups i.e., 50–64 (early) (CN = 300, CI = 29, and CI-AD = 58), 65–70 (intermediate) (CN = 560, CI = 107, and CI-AD = 314), and ≥80 (late) (CN = 222, CI = 61, and CI-AD = 216). The lower the *t* value, the higher the difference in the lateral ventricle volume between the cognitive groups. The t-value significance was set at $p < 0.017$ (Bonferroni corrected) and the color bar depicts the *t* value. Early enlargement of the ventricles was observed for CI and CI-AD groups compared to the CN. **B**, **C** Lateral Ventricle and CSF volume of CN, CI, and CI-AD subjects across early, intermediate, and late age groups respectively. *P* values were calculated with the unpaired, two-tailed Welch's *t* test followed by Bonferroni correction. Statistical significance for comparing the mean lateral ventricle and CSF volume among cognitive groups (CN, CI, and CI-AD) across the stratified age groups was depicted as $*p < 0.017$, $**p < 0.001$. **D**, **E** LME model regression analysis of Lateral ventricle volume and CSF shows a progressive increase in the volume across three cognitive groups- CN (green), CI (blue), and CI-AD (red). The LME analysis was performed upon setting up the age intercept at 50 years. Statistical significance for the slope and intercept comparison between CN vs CI (*), CN vs CI-AD ($^{\#}$), and CI vs CI-AD ($^{\$}$) was set at $p < 0.05$.

accuracy with other ML algorithms, Simple Classification tree provided an average accuracy of 80.7 ± 1.9%, while Random Forest achieved average accuracy of 83.7 ± 1.2% (Fig. 5B).

Establishing brain age using 180 MRI-determined volumetry features

This unique Brain age estimation model utilizing the 178 neuroanatomic volumetry and two WMH (PVWMH and DWMH) volumes provided significantly and strongly correlated BA with CA (average correlation coefficient (*r*) as 0.89 ± 0.03 for 50 iterations) suggestive of a reliable and robust architecture of the BA estimation model (Fig. 6). BA was not significantly different from CA for the CN subjects with low WMH. BAG, determined by subtracting the CA from BA, revealed that CN subjects who had high WMH (5–10 ml) load in the brain were estimated to have significantly higher BAG at the early (2.5 ± 2.9 years, $p < 0.001$) and intermediate age groups (2.2 ± 3.3 years, $p < 0.001$) compared to the subjects with undetectable or low WMH (<1.5 ml) (Fig. 6, Supplementary Fig. 5A). Further, cross-validation for the estimation of BA using the same model architecture using the ADNI-3 cohort, revealed similar BAG estimates as for the NACC cohort for the subjects with no and high WMH load (Supplementary Fig. 5B).

Permutation importance analyses for the top ten brain volumetry contributors towards BA estimation for the subjects with no WMH revealed that the volume of 3rd ventricle is the topmost feature with an importance factor of 0.14 (Supplementary Fig. 6A) while, for the subjects with high WMH, the volume of periventricular white matter hyperintensity (PVWMH) was the most important feature with an importance factor of 0.083 (Supplementary Fig. 6B). However, a set of brain structures; the volume of accumbens area, the ratio of brain segmented volume by total intracranial volume, and amygdala are common top features contributing towards brain age for both the groups *viz* no WMH and high WMH, but the extent of contribution is distinct. It is noticeable that in the case of high WMH subjects, PVWMH contributes maximally to the BA compared to DWMH (0.083 vs 0.002).

DISCUSSION

Quantification of chronological aging-associated changes in the magnitude of neuroanatomic volume, temporal sequence (early, intermediate, and late), and WMH load is imperative to develop a non-invasive quantitative precise clinical index for ascertaining the brain health and cognitive status. The brain structural changes in CN, CI, and CI-AD subjects were compared for the three age groups to identify early, intermediate, and late brain MRI events in the trajectory of aging. Using the brain MRI quantified features, a ML model was established to pinpoint an optimal but minimum number of brain MRI-segmented features discriminative of cognitive status. Moreover, for the first time a comprehensive brain age (BA) model was developed using the neuroanatomic structures together with periventricular and deep WMH volume for estimating the BA and BAG (Supplementary Fig. 1).

Hippocampal volume quantification in CI and CI-AD subjects is not distinctive of CI and CI-AD at early age groups. The early onset of AD (EOAD) i.e., before the age of 65, presents with a non-amnestic phenotype that spares the involvement of hippocampi [44, 45], is in consistence with the findings of no significant difference in hippocampus, GM, and WM volume between CI and CI-AD subjects at the early age groups. The substantial loss in the hippocampus provides sensitivity to differentiate between CI and CI-AD at the intermediate age group of ≥65 years, at which almost

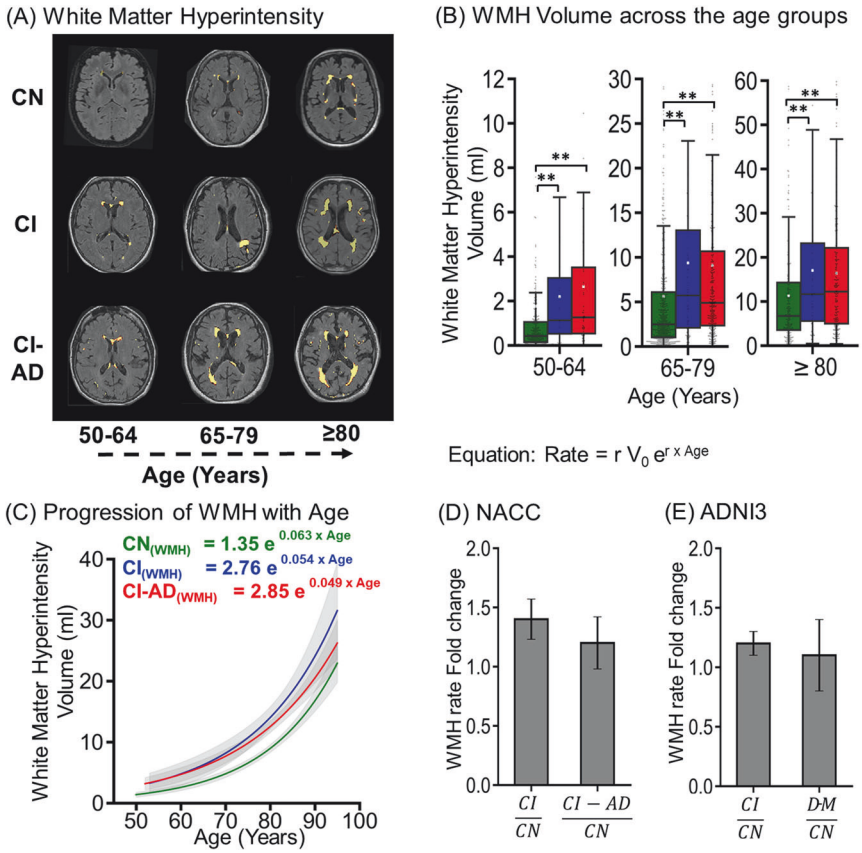

Fig. 4 White matter hyperintensity (WMH) loads across CN, CI, and CI-AD subjects. A Segmentation mask of WMH load generated from T1w, and T2-FLAIR MRI for CN CI and CI-AD subjects across early, intermediate, and late age groups. **B** The Boxplot depicts the median (solid line) and the mean (white square) WMH volume across 50–64 (early) (CN = 300, CI = 29, and CI-AD = 58), 65–79 (intermediate) (CN = 560, CI = 107, and CI-AD = 314), and ≥80 (late) (CN = 222, CI = 61, and CI-AD = 216) subjects. *p* values were calculated with the Mann-Whitney U test followed by Bonferroni correction. Statistical significance for the WMH comparison among cognitive groups (CN, CI, and CI-AD) across the age groups was depicted as $*p < 0.017$, $**p < 0.001$. **C** The exponential increase of total WMH load with age across CN (green), CI (blue), and CI-AD (red) subjects. The equation represents the rate of change of WMH load where, *r* is the rate constant and V_0 is the initial WMH volume at 50 years of age. **D** Bar plot depicting mean ± standard deviation WMH rate fold change for CI and CI-AD subjects with respect to cognitively normal (CN) subjects in NACC cohort. **E** Bar plot depicting Average WMH rate fold change in CI and Dementia (DM) subjects with respect to CN subjects in ADNI cohort.

94% of late-onset of AD cases are observed and become symptomatic.

Interestingly, quantification of thinning of PHG provided one of the unique early age changes discriminative of CI vs CI-AD. Indeed, the medial lobe cortices are the primary site for tau deposition, a key characteristic in the manifestation of Alzheimer's disease. Indeed, the prior measurements of parahippocampal cortical thickness in a community cohort reported parahippocampal thinning as one of the most important features of amnestic (Mild cognitive) MCI and AD [46, 47]. The entorhinal cortical (EC) thickness was discriminative of CI and CI-AD subjects at the intermediate age group but failed to distinguish CN vs CI and CI vs CI-AD at the early age groups, suggests EC thinning is not an early event in manifestation of CI and CI-AD. However, the thinning of EC in CI and CI-AD compared to CN is significantly noticeable at the intermediate and late age groups. A prior study that measured EC thickness did not observe significant differences between CN and amnestic (mild cognitively impaired) MCI [47], as it did not stratify the thickness for age groups but rather pooled the EC measurements across a large age range.

Similar to the trends observed for PHG, quantification of CSF volume also provided an early feature discriminative of CI from CI-AD. Since CSF volume was not distinct in CI compared to CN at the early age group, thus CSF quantification may not be a sensitive feature for early age discrimination of CI and CN. But, the quantification of lateral ventricles provided sensitivity for an early discrimination of CI vs CN and CI-AD vs CN subjects (Supplementary Table 3, 5). This indicates that a combination of CSF and ventricular volume must be analyzed together to pinpoint the early chronological aging changes to discern CN, CI, and CI-AD groups.

Quantitative estimation of GM and WM at early age provides significant sensitivity for delineation of CI and CI-AD subjects from that of CN but fails to distinguish between CI and CI-AD subjects at the early age group. A reduced rate of GM and WM atrophy in the CI and CI-AD subjects was observed in contrast to prior reports of the increased rate of loss of GM and WM in AD subjects compared to the healthy controls [48–50]. Here, we argue that, since the CI and CI-AD subjects present with significantly lower volume at the baseline measurements (50 years of age) compared to the CN, in no condition, CI and CI-AD will have a faster rate of atrophy compared to the CN. The slower rate of change of GM and WM volume is solely attributed to lower baseline values of GM and WM. Therefore, absolute volumetric quantification of neuroanatomic volume at a given age is mandatory while evaluating the structural kinetics in longitudinal measurements.

Progressive increase in WMH load with aging across all the three cognitive groups CN, CI, and CI-AD is suggestive of enhanced vascular insult to neuroanatomic structures, which is likely to trigger an accelerated aging-associated neuroanatomic

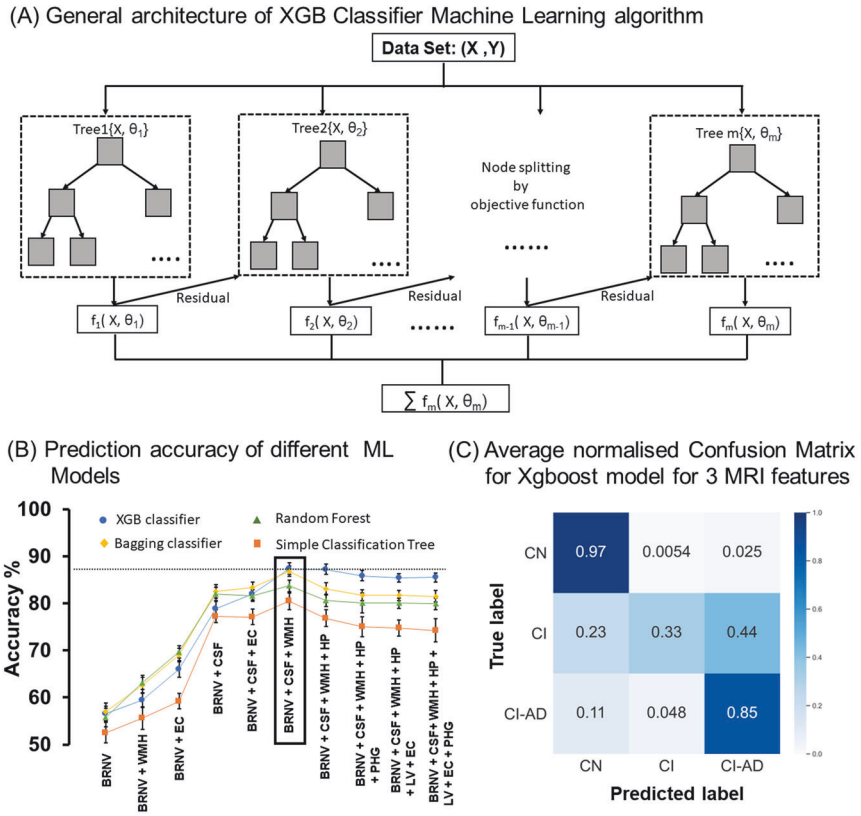

Fig. 5 Summary of the Machine learning algorithm performance in predicting the cognitive status of the participants based on the MRI-segmented brain volume and thickness and age. A Schematics of XGB classifier ML model based on the gradient boosting technique. **B** Cognitive status prediction accuracy of different ML Models for combination of different MRI obtains neuroanatomic volumes and thicknesses. MRI features were added one by one with age and gender to check for the increase in average accuracy of XGB classifier (blue circle), Random Forest (green triangle), Bagging classifier (yellow diamond) and Simple Classification Tree (orange square) ML models. The result showed the mean accuracy ± SD (standard deviation). The highest accuracy for all ML models was obtained for the combination of three MRI features, i.e., total Brain volume, CSF, and WMH with age and gender, and out of the 4 ML models, the XGB classifier gave the highest accuracy. **C** Average normalized confusion matrix for XGB classifier ML machine models for predicting the cognitive status of the test data for the three optimized MRI features (total brain volume, CSF, and WMH) with age and gender, which gave the highest accuracy. *BRNV total brain volume, CSF cerebrospinal fluid, LV lateral ventricle, HP hippocampus, WMH white matter hyperintensity, EC entorhinal cortex and PHG parahippocampal gyrus.

changes thus predisposing altered structure-function relationship and transforming the aging trajectory towards CI and/or CI-AD. Indeed, a two-fold rate of WMH increase in CI and CI-AD compared to CN with aging is plausibly the cause of early and remarkable neuroanatomic volumetry deterioration in CI and CI-AD subjects. Since WMH load is increased in both CI and CI-AD but is not different between CI and CI-AD subjects, is suggestive of a similar vascular involvement in CI and CI-AD subjects. An exponential increase in WMH load indicates that once the punctate WMH lesions attain confluency at an age, an abrupt WMH increase is observed leading to an exponential pattern of increase.

Volumetry comparisons at the early, intermediate, and late age groups (Supplementary Table 3, 5) revealed that the volume of GM, WM, HP, BRNV, CSF, LV are significantly altered in CI and CI-AD subjects compared to CN at early age groups but only medial cortical thinning and increase in CSF volume mark an early event depictive of clinical manifestation of CI and CI-AD. Indeed, not all brain structures may serve as a discriminator for cognitive status, as the magnitude of changes is subtle, and follows a unique sequence which are temporally and spatially separated, Therefore, in order to attain clinical suitability, it is impeccable to deduce the minimum number of optimal, unique, easy-to-quantify MRI features distinctive of cognitive health. The ML models establish a significantly higher accuracy for predicting cognitive status using a minimum number of three distinct features comprising a structural feature, i.e., the total brain volume (=GM and WM), a glymphatic system as CSF volume, and a small vessel disease feature, i.e., WMH. The inclusion of additional MRI-determined neuroanatomical structures did not improve the accuracy and led to plateauing of the accuracy, suggesting the ease of extension of our current findings across various aging cohorts and clinical validations in the decision-making of cognitive status using structural and small vessel disease load. Given the WMH presence in almost all the brains studied in this study across CN, CI, and CI-AD in minuscule or high amounts, WMH quantification and its inclusion with neuroanatomic volume is unavoidable to study aging-associated brain health. The ML model clearly indicates that WMH volume is one of the unique features along with total brain volume and CSF, as a predictor of clinical cognitive status. WMH quantitation, along with structural volumetry, will provide the extent of vascular insult and its impact on the structure and functional status of the brain.

Our BA estimation model is a unique study wherein the WMH load of PVWMH and DWMH have been included together with neuroanatomic features. The subjects with low and high WMH revealed a clearly distinct higher BAG. Subjects with WMH > 5 ml had BAG of more than ~3 years compared to the subjects with low or minuscule WMH. This study firmly establishes a strong perspective that in order to understand the normal aging and pathological aging trajectory, it is mandatory to account for WMH

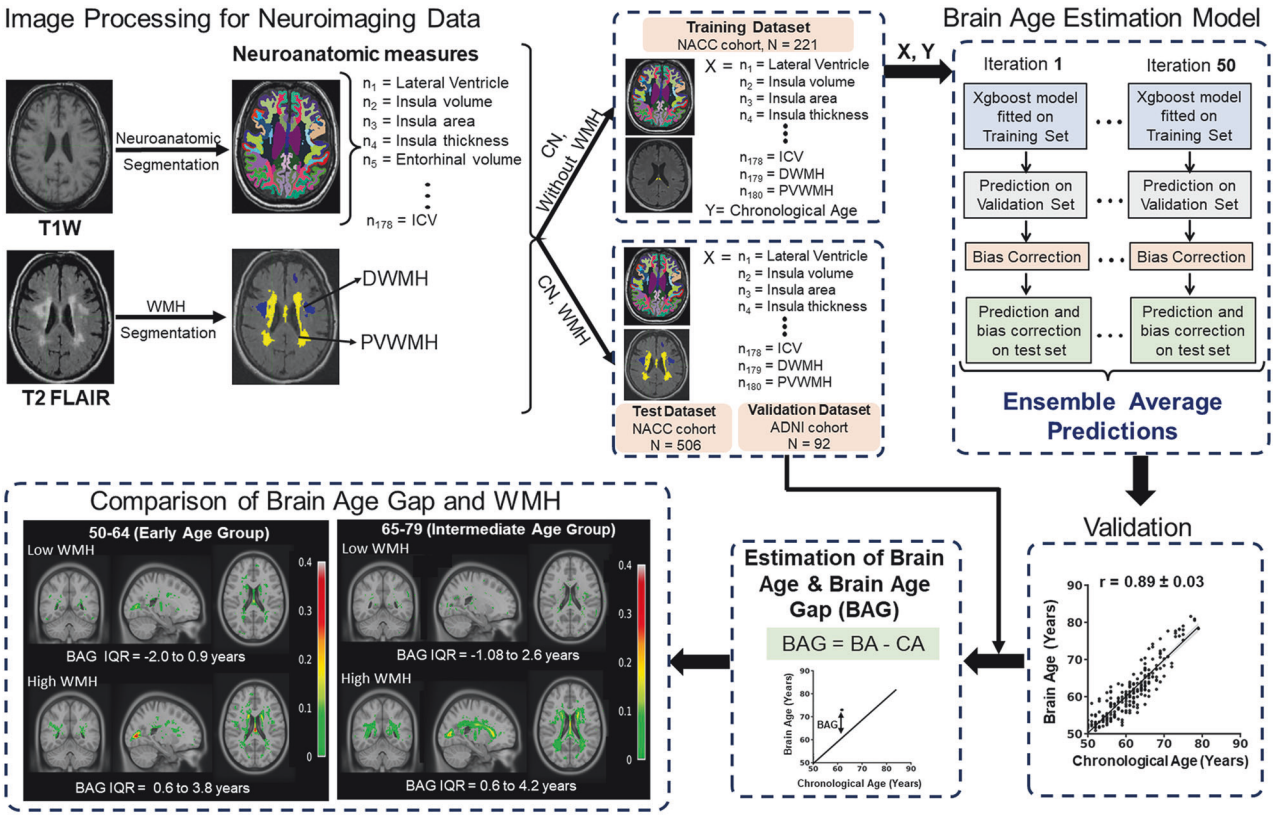

Fig. 6 Brain age (BA) model developed from 180 MRI-obtained neuroanatomical volumetry and white matter hyperintensity load. Schematics illustrating the workflow of the Brain Age estimation model. The T1 and T2-FLAIR MR images from CN subjects were segmented to obtain 178 neuroanatomic measures, PVWMH, and DWMH. The subjects were then divided into training, test, and validation data sets. The neuroanatomic features, PVWM and DWMH of the subjects in the training data set were used as an input together with Chronological Age (CA) to develop the BA model. The model's performance was validated using the average association between BA and CA, obtained from the average prediction for 50 iterations. BA and Brain Age Gap (BAG) were estimated using the BA model for test and validation data sets. A comparison of BAG and WMH was shown using voxel-wise probability maps, depicting the occurrence of total WMH load (PVWMH + DWMH) on the coronal, sagittal and axial slice for cognitively normal subjects in the early age group with no or low WMH (WMH < 1.5 ml, $n = 95$) and high WMH (WMH 5–10 ml, $n = 32$) and intermediate age group with no or low WMH ($n = 35$) and high WMH ($n = 118$) with the range of BAG.

load and cannot treat the subjects with WMH and without WMH together. Owing to the vascular insult from WMH, the structural atrophy and hypertrophy kinetics will be distinct depending upon WMH load. Gray matter (Neuronal body) and white matter (fiber) loss is an early event of compromised structural health, and beyond a threshold of WMH load when it tips up suddenly, the GM and WM loss may get accelerated resulting in accelerated cognitive decline, and hence increased BAG. Our BA estimation model showed a strong correlation between BA estimates and CA ($r = 0.89 \pm 0.03$), aligning closely with prior studies [51]. The ML model for determining the optimal features for cognitive discrimination is robust and reliable given the cross-validation of the ML model was iterated six times with non-overlapping training in such a fashion that no data gets repeated, but all the data sets serve as part of training during one or the other iteration data and thus minimize any outcome arising because of overfitting. Cross-validation results strongly claim that our model would perform reliably on any prospective or retrospective neuroanatomic and WMH measurements in aging cohorts. Furthermore, the rate of structural changes obtained from LME-based longitudinal data analysis removes the individual variabilities arising from the distinct age of entry of subjects during the study. However, linear regression using cross-sectional measurements viz quantification from the first visit (Supplementary Fig. 4, Supplementary Table 4B) depicts a similar slope and pattern as obtained from longitudinal measurements. Given the ease of designing cross-sectional studies, finding similar kinetics and temporal patterns as that obtained from longitudinal measurements is encouraging for extensive aging studies at multiple sites.

BA is indeed a comprehensive representation of a set of neuroanatomical quantities which are major contributors, such as 3rd Ventricle volume estimates with chronological aging contributes most towards BA with an importance factor of 0.14 out of the top 10 brain features such as volume of accumbens, brain segmented volume by total intracranial volume ratio, amygdala volume, post-central thickness, cerebellum white matter volume, caudal-anterior cingulate white matter volume, posterior cingulate surface area, temporal pole white matter volume, and post-central white matter volume (Supplementary Fig. 6A). It is interesting to further enhance the biological underpinning of these top 10 features which appears to be key players for BA and brain health in the subjects with no WMH deposition. It is intriguing to note that a unique set of brain features contributes towards the BA for the subjects with high WMH load compared to the low/nil WMH subjects (Supplementary Fig. 6B). Despite the differences in the set of important features between the two groups, a few features were common contributors of the BA estimation. Therefore, here we establish that BAG may serve as a potential clinical measure of brain health, when investigated into structural and commonly observed small vessel pathology of WMH. The findings from our study strongly claim that the ongoing and prospective aging and AD consortium investigations must revisit the role of small vessel diseases, develop a common pipeline and method to quantify WMH together with structural,

cognitive, and vascular variables to precisely delineate the clinical and biological roles of WMH for improved understanding of aging-associated disorders.

CONCLUSION

'Three' unique brain changes associated with aging, wherein two structural features, Total brain volume, and CSF volume, together with WMH lesion load provide highly precise discrimination of cognitive status as CN, CI, and CI-AD. The unique brain age model that incorporates WMH load, for the first time, along with neuroanatomic quantities, depicts that the elevated load of WMH at a given CA contributes to an increased BAG even in subjects identified as CN using cognitive batteries. Despite the presence of a structural lesion in the form of WMH in the brain, an individual gets classified as CN, calling for a debate on the precision of the clinical cognitive evaluations as a true indicator of brain health. Increased BAG with elevated WMH load, even at the early age group is suggestive of profound vascular insult resulting in early and accelerated neuroanatomic atrophy or hypertrophy. Cross-validation in the ADNI cohort provided a similar increase in BAG in the subjects with elevated WMH load. Our sample size had the subjects only starting at the age of 50 years. Further extension of our study analyses to a retrospective or prospective cohort that includes a younger group of subjects <50 years of age will provide comprehensive insights into the role of WMH in chronological aging and application of the Brain age model.

While the loss of hippocampus volume, GM and WM volume is distinctive of CI and CI-AD from CN at the early age group but lacks sensitivity to discriminate between CI and CI-AD. It is remarkable to note that medial cortical thinning from the parahippocampal gyrus is an Early event discriminative of CI from that of CI-AD. It is very evident that quantification of WMH along with neuroanatomic structural features provide a quantitative and sequential platform with a sensitivity for early, intermediate, and late age delineation of the cognitive status. An early and substantial loss of GM, WM, HP, EC, and PHG in CI and CI-AD subjects is likely to be a manifestation of high WMH load and increased progression kinetics in CI and CI-AD subjects. Indeed, WMH serves as one of the three unique features discriminative of cognitive status and also estimates of PVWMH load as a significant contributor towards increased BAG. Henceforth, this study establishes that quantification of WMH together with an optimal number of neuroanatomic features is mandatory to delve into the biological underpinning of aging and aging-associated cognitive disorders.

DATA AVAILABILITY

Data used in the current study are available through the NACC (naccdata.org) and the ADNI website (https://adni.loni.usc.edu). Detailed data analysis plan and syntax will be made available upon request to the corresponding author.

CODE AVAILABILITY

The Volumetry data and the codes used for comparison of volumetry, ML models for optimizing the Brain features discriminative of cognitive status, and Brain Age estimation model are uploaded in the GitHub repository (https://github.com/nibr-lab/TP-2024_manuscript-code).

REFERENCES

1. Stephan Y, Sutin AR, Luchetti M, Terracciano A. Subjective age and risk of incident dementia: evidence from the National Health and Aging Trends survey. J Psychiatr Res. 2018;100:1–4.
2. Dickerson BC, Stoub TR, Shah RC, Sperling RA, Killiany RJ, Albert MS, et al. Alzheimer-signature MRI biomarker predicts AD dementia in cognitively normal adults. Neurology. 2011;76:1395–402.
3. Kaye JA, Swihart T, Howieson D, Dame A, Moore MM, Karnos T, et al. Volume loss of the hippocampus and temporal lobe in healthy elderly persons destined to develop dementia. Neurology. 1997;48:1297–304.
4. Peters R. Ageing and the brain. Postgrad Med J. 2006;82:84–88.
5. Raz N. Selective aging of the human cerebral cortex observed in vivo: differential vulnerability of the prefrontal gray matter. Cereb Cortex. 1997;7:268–82.
6. Scahill RI, Frost C, Jenkins R, Whitwell JL, Rossor MN, Fox NC. A longitudinal study of brain volume changes in normal aging using serial registered magnetic resonance imaging. Arch Neurol. 2003;60:989.
7. Suzuki H, Venkataraman AV, Bai W, Guitton F, Guo Y, Dehghan A, et al. Associations of regional brain structural differences with aging, modifiable risk factors for dementia, and cognitive performance. JAMA Netw Open. 2019;2:e1917257.
8. Taki Y, Kinomura S, Sato K, Goto R, Kawashima R, Fukuda H. A longitudinal study of gray matter volume decline with age and modifying factors. Neurobiol Aging. 2011;32:907–15.
9. Trollor JN, Valenzuela MJ. Brain ageing in the new millennium. Aust NZ J Psychiatry. 2001;35:788–805.
10. Wardlaw JM, Valdés Hernández MC, Muñoz-Maniega S. What are white matter hyperintensities made of? J Am Heart Assoc 2015;4:001140.
11. Albert MS, DeKosky ST, Dickson D, Dubois B, Feldman HH, Fox NC, et al. The diagnosis of mild cognitive impairment due to Alzheimer's disease: Recommendations from the National Institute on Aging-Alzheimer's Association workgroups on diagnostic guidelines for Alzheimer's disease. Alzheimer's Dement. 2011;7:270–9.
12. Chen Y-X, Liang N, Li X-L, Yang S-H, Wang Y-P, Shi N-N. Diagnosis and treatment for mild cognitive impairment: a systematic review of clinical practice guidelines and consensus statements. Front Neurol 2021;12:719849.
13. Hugo J, Ganguli M. Dementia and cognitive impairment. Clin Geriatr Med. 2014;30:421–42.
14. Langa KM, Levine DA. The diagnosis and management of mild cognitive impairment. JAMA. 2014;312:2551.
15. McKhann GM, Knopman DS, Chertkow H, Hyman BT, Jack CR, Kawas CH, et al. The diagnosis of dementia due to Alzheimer's disease: Recommendations from the National Institute on Aging-Alzheimer's Association workgroups on diagnostic guidelines for Alzheimer's disease. Alzheimer's Dement. 2011;7:263–9.
16. Nosheny RL, Camacho MR, Insel PS, Flenniken D, Fockler J, Truran D, et al. Online study partner-reported cognitive decline in the Brain Health Registry. Alzheimer's Dement: Transl Res Clin Interv. 2018;4:565–74.
17. Rueda AD, Lau KM, Saito N, Harvey D, Risacher SL, Aisen PS, et al. Self-rated and informant-rated everyday function in comparison to objective markers of Alzheimer's disease. Alzheimer's Dement. 2015;11:1080–9.
18. Kumar Gupta N, Yadav N, Aman A, Tiwari V. Brain WMH Load, kinetics and regional distribution with aging: a signature of structural and cognitive health. International Society for Magnetic Resonance in Medicine, 2003.
19. Yadav N, Majumdar A, Tiwari V. MRI measured neuroanatomic volume, cortical thinning and Wmh load with aging: the early, intermediate and late events of cognitive status. In: Imaging Aging, Dementia & Alzheimer's Disease I. International Society for Magnetic Resonance in Medicine, 2003.
20. Beekly DL, Ramos EM, Lee WW, Deitrich WD, Jacka ME, Wu J, et al. The National Alzheimer's Coordinating Center (NACC) Database: The Uniform Data Set. Alzheimer Dis Assoc Disord. 2007;21:249–58.
21. Beekly DL, Ramos EM, van Belle G, Deitrich W, Clark AD, Jacka ME, et al. The National Alzheimer's Coordinating Center (NACC) Database: an Alzheimer disease database. Alzheimer Dis Assoc Disord. 2004;18:270–7.
22. Besser L, Kukull W, Knopman DS, Chui H, Galasko D, Weintraub S, et al. Version 3 of the National Alzheimer's Coordinating Center's Uniform Data Set. Alzheimer Dis Assoc Disord. 2018;32:351–8.
23. Müller H-P, Huppertz H-J, Dreyhaupt J, Ludolph AC, Tabrizi SJ, Roos RAC, et al. Combined cerebral atrophy score in Huntington's disease based on atlas-based MRI volumetry: sample size calculations for clinical trials. Parkinsonism Relat Disord. 2019;63:179–84.
24. Thota SM, Chan KL, Pradhan SS, Nagabushana B, Priyanka GB, Sunil HV, et al. Multimodal imaging and visual evoked potentials reveal key structural and functional features that distinguish symptomatic from presymptomatic Huntington's disease Brain. Neurol India. 2021;69:1247–58.
25. Bates D, Mächler M, Bolker B, Walker S. Fitting linear mixed-effects models using lme4. J Stat Softw 2015;67:1–48.
26. R Core Team. R: a language and environment for statistical computing. 2021.
27. Alexopoulos EC. Introduction to multivariate regression analysis. Hippokratia. 2010;14:23–8.
28. Shafer AT, Williams OA, Perez E, An Y, Landman BA, Ferrucci L et al. Accelerated decline in white matter microstructure in subsequently impaired older adults and its relationship with cognitive decline. Brain Commun 2022;4:fcac051.

29. Cook AH, Sridhar J, Ohm D, Rademaker A, Mesulam M-M, Weintraub S, et al. Rates of cortical atrophy in adults 80 years and older with superior vs average episodic memory. JAMA. 2017;317:1373.
30. Geifman N, Cohen R, Rubin E. Redefining meaningful age groups in the context of disease. Age (Omaha). 2013;35:2357–66.
31. Burchett WW, Ellis AR, Harrar SW, Bathke AC. Nonparametric inference for multivariate data: the *R* Package npmv. J Stat Softw 2017;76:1–18.
32. Alosco ML, Sugarman MA, Besser LM, Tripodis Y, Martin B, Palmisano JN, et al. A clinicopathological investigation of white matter hyperintensities and Alzheimer's disease neuropathology. J Alzheimer's Dis. 2018;63:1347–60.
33. Jiang J, Liu T, Zhu W, Koncz R, Liu H, Lee T, et al. UBO detector – a cluster-based, fully automated pipeline for extracting white matter hyperintensities. Neuroimage. 2018;174:539–49.
34. Pedregosa F, Varoquaux G, Gramfort A, Michel V, Thirion B, Grisel O, et al. Scikit-learn: machine learning in Python. J Mach Learn Res. 2011;12:2825–30.
35. Amr T. Hands-on machine learning with scikit-learn and scientific Python toolkits: a practical guide to implementing supervised and unsupervised machine learning algorithms in Python. Packt Publishing, Limited: Birmingham,UK, 2020.
36. Charbuty B, Abdulazeez A. Classification based on decision tree algorithm for machine learning. J Appl Sci Technol Trends. 2021;2:20–28.
37. Breiman L. Random Forests. Mach Learn. 2001;45:5–32.
38. Breiman L. Bagging predictors. Mach Learn. 1996;24:123–40.
39. González S, García S, Del Ser J, Rokach L, Herrera F. A practical tutorial on bagging and boosting based ensembles for machine learning: Algorithms, software tools, performance study, practical perspectives and opportunities. Inf Fusion. 2020;64:205–37.
40. Chen T, Guestrin C XGBoost. In: Proceedings of the 22nd ACM SIGKDD International Conference on Knowledge Discovery and Data Mining. ACM: New York, NY, USA, 2016, pp 785–94.
41. Tougui I, Jilbab A, Mhamdi JE. Impact of the choice of cross-validation techniques on the results of machine learning-based diagnostic applications. Health Inf Res. 2021;27:189–99.
42. Fischl B. FreeSurfer. Neuroimage. 2012;62:774–81.
43. Baecker L, Garcia-Dias R, Vieira S, Scarpazza C, Mechelli A. Machine learning for brain age prediction: introduction to methods and clinical applications. EBioMedicine. 2021;72:103600.
44. Mendez MF. Early-onset Alzheimer disease and its variants. Continum. 2019;25:34–51.
45. Phillips ML, Stage EC Jr, Lane KA, Gao S, Risacher SL, Goukasian N, et al. Neurodegenerative patterns of cognitive clusters of early-onset Alzheimer's disease subjects: evidence for disease heterogeneity. Dement Geriatr Cogn Disord. 2019;48:131–42.
46. Krumm S, Kivisaari SL, Probst A, Monsch AU, Reinhardt J, Ulmer S, et al. Cortical thinning of parahippocampal subregions in very early Alzheimer's disease. Neurobiol Aging. 2016;38:188–96.
47. Machulda MM, Lundt ES, Albertson SM, Spychalla AJ, Schwarz CG, Mielke MM, et al. Cortical atrophy patterns of incident MCI subtypes in the mayo clinic study of aging. Alzheimer's Dement. 2020;16:1013–22.
48. Mak E, Su L, Williams GB, Watson R, Firbank M, Blamire AM, et al. Longitudinal assessment of global and regional atrophy rates in Alzheimer's disease and dementia with Lewy bodies. Neuroimage Clin. 2015;7:456–62.
49. Sluimer JD, van der Flier WM, Karas GB, Fox NC, Scheltens P, Barkhof F, et al. Whole-brain atrophy rate and cognitive decline: longitudinal MR study of memory clinic patients. Radiology. 2008;248:590–8.
50. Whitwell JL, Jack CR, Parisi JE, Knopman DS, Boeve BF, Petersen RC, et al. Rates of cerebral atrophy differ in different degenerative pathologies. Brain. 2006;130:1148–58.
51. Franke K, Gaser C. Ten years of BrainAGE as a neuroimaging biomarker of brain aging: what insights have we gained? Front Neurol 2019;10:789.

ACKNOWLEDGEMENTS

The Brain age estimation model was established using neuroanatomic data from the National Alzheimer's Coordinating Center (NACC). The Brain age modeling and the estimation of BAG was cross-validated using the data from Alzheimer's Disease Neuroimaging Initiative (ADNI). The NACC database is funded by NIA/NIH Grant U24 AG072122. NACC data are contributed by the NIA-funded ADRCs: P30 AG062429 (PI James Brewer, MD, PhD), P30 AG066468 (PI Oscar Lopez, MD), P30 AG062421 (PI Bradley Hyman, MD, PhD), P30 AG066509 (PI Thomas Grabowski, MD), P30 AG066514 (PI Mary Sano, PhD), P30 AG066530 (PI Helena Chui, MD), P30 AG066507 (PI Marilyn Albert, PhD), P30 AG066444 (PI John Morris, MD), P30 AG066518 (PI Jeffrey Kaye, MD), P30 AG066512 (PI Thomas Wisniewski, MD), P30 AG066462 (PI Scott Small, MD), P30 AG072979 (PI David Wolk, MD), P30 AG072972 (PI Charles DeCarli, MD), P30 AG072976 (PI Andrew Saykin, PsyD), P30 AG072975 (PI David Bennett, MD), P30 AG072978 (PI Neil Kowall, MD), P30 AG072977 (PI Robert Vassar, PhD), P30 AG066519 (PI Frank LaFerla, PhD), P30 AG062677 (PI Ronald Petersen, MD, PhD), P30 AG079280 (PI Eric Reiman, MD), P30 AG062422 (PI Gil Rabinovici, MD), P30 AG066511 (PI Allan Levey, MD, PhD), P30 AG072946 (PI Linda Van Eldik, PhD), P30 AG062715 (PI Sanjay Asthana, MD, FRCP), P30 AG072973 (PI Russell Swerdlow, MD), P30 AG066506 (PI Todd Golde, MD, PhD), P30 AG066508 (PI Stephen Strittmatter, MD, PhD), P30 AG066515 (PI Victor Henderson, MD, MS), P30 AG072947 (PI Suzanne Craft, PhD), P30 AG072931 (PI Henry Paulson, MD, PhD), P30 AG066546 (PI Sudha Seshadri, MD), P20 AG068024 (PI Erik Roberson, MD, PhD), P20 AG068053 (PI Justin Miller, PhD), P20 AG068077 (PI Gary Rosenberg, MD), P20 AG068082 (PI Angela Jefferson, PhD), P30 AG072958 (PI Heather Whitson, MD), P30 AG072959 (PI James Leverenz, MD).Data collection and sharing for the ADNI data was funded by the Alzheimer's Disease Neuroimaging Initiative (ADNI) (National Institutes of Health Grant U01 AG024904) and DOD ADNI (Department of Defense award number W81XWH-12-2-0012). ADNI is funded by the National Institute on Aging, the National Institute of Biomedical Imaging and Bioengineering, and through generous contributions from the following: AbbVie, Alzheimer's Association; Alzheimer's Drug Discovery Foundation; Araclon Biotech; BioClinica, Inc.; Biogen; Bristol-Myers Squibb Company; CereSpir, Inc.; Cogstate; Eisai Inc.; Elan Pharmaceuticals, Inc.; Eli Lilly and Company; EuroImmun; F. Hoffmann-La Roche Ltd and its affiliated company Genentech, Inc.; Fujirebio; GE Healthcare; IXICO Ltd.; Janssen Alzheimer Immunotherapy Research & Development, LLC.; Johnson & Johnson Pharmaceutical Research & Development LLC.; Lumosity; Lundbeck; Merck & Co., Inc.; Meso Scale Diagnostics, LLC.; NeuroRx Research; Neurotrack Technologies; Novartis Pharmaceuticals Corporation; Pfizer Inc.; Piramal Imaging; Servier; Takeda Pharmaceutical Company; and Transition Therapeutics. The Canadian Institutes of Health Research is providing funds to support ADNI clinical sites in Canada. Private sector contributions are facilitated by the Foundation for the National Institutes of Health (www.fnih.org). The grantee organization is the Northern California Institute for Research and Education, and the study is coordinated by the Alzheimer's Therapeutic Research Institute at the University of Southern California. ADNI data are disseminated by the Laboratory for Neuro Imaging at the University of Southern California. We also acknowledge the contribution of Mr. V. Ashwin and Mr. Arkaprava Majumdar for helping in ML methods.

AUTHOR CONTRIBUTIONS

VT and NY conceptualized and designed the study; NY, NKG, and VT analyzed the data, and contributed to data interpretation; DT contributed to initial data analysis; NY and VT drafted the manuscript. All authors reviewed the results and approved the final version of the manuscript.

COMPETING INTERESTS

The authors declare no competing interests.

ETHICS APPROVAL AND CONSENT TO PARTICIPATE

ADRCs have been contributing data to the UDS at NACC since 2005 [20–22], including participants with cognitive status ranging from no cognitive impairment to dementia. The ADRCs obtain the written informed consent from the participants based on the IRB approval of each ADRCs (https://naccdata.org/requesting-data/nacc-data). All NACC data is freely available to researchers. To receive the NACC data a request is submitted by the user (https://naccdata.org/requesting-data/data-request-process). For the present study, we at IISER Berhampur received anonymized UDS and MRI from the NACC ADRCs (Data Request ID #5530) on 22 October 2021, for our analysis.

ADDITIONAL INFORMATION

Supplementary information The online version contains supplementary material available at https://doi.org/10.1038/s41398-024-03097-2.

Correspondence and requests for materials should be addressed to Vivek Tiwari.

Reprints and permission information is available at http://www.nature.com/reprints

Publisher's note Springer Nature remains neutral with regard to jurisdictional claims in published maps and institutional affiliations.